



ELSEVIER

Available online at [www.sciencedirect.com](http://www.sciencedirect.com)

ScienceDirect

journal homepage: [www.elsevier.com/locate/he](http://www.elsevier.com/locate/he)

# Ni–Cu/Ce<sub>0.9</sub>Zr<sub>0.1</sub>O<sub>2</sub> bimetallic cermets for electrochemical and catalytic applications

Lucía M. Toscani<sup>a</sup>, M. Genoveva Zimicz<sup>a,b</sup>, Jorge R. Casanova<sup>a</sup>,  
Susana A. Larrondo<sup>a,c,\*</sup>

<sup>a</sup>CINSO (Centro de Investigaciones en Sólidos), UNIDEF – CONICET, J.B. de La Salle N°4397, 1603 Villa Martelli, Pcia. de Buenos Aires, Argentina

<sup>b</sup>Instituto de Física del Sur – CONICET, Av. Alem N°1253, 8000 Bahía Blanca, Pcia. de Buenos Aires, Argentina

<sup>c</sup>Departamento de Ingeniería Química, Facultad de Ingeniería, Universidad de Buenos Aires, Pabellón de Industrias, Ciudad Universitaria, 1428 Buenos Aires, Argentina

## ARTICLE INFO

### Article history:

Received 17 October 2013

Accepted 5 December 2013

Available online 31 December 2013

### Keywords:

CeO<sub>2</sub>–ZrO<sub>2</sub>

IT-SOFCs

Anodes

Electrocatalytic activity

Methane partial oxidation

## ABSTRACT

The development of an economically feasible Solid Oxide Fuel Cell technology has driven the research activity in this area toward the reduction of their operating temperature. New anode materials, with high electrocatalytic activity and resistance to coke deposition when hydrocarbons are used as fuel, have to be developed. The aim of this paper is to give a contribution in this area by studying the effect of Ni substitution by Cu in the NiO (60 wt.)/Ce<sub>0.9</sub>Zr<sub>0.1</sub>O<sub>2</sub> cermet recently proposed as a possible anode material.

It was observed that the partial replacement of Ni by Cu has produced solids with high reducibility, excellent catalytic and electrocatalytic performances and higher resistance to carbon deposition in the operation with CH<sub>4</sub>.

Copyright © 2013, Hydrogen Energy Publications, LLC. Published by Elsevier Ltd. All rights reserved.

## 1. Introduction

The development of Solid Oxide Fuel Cell (SOFC) technology has become important in the last years due to the need to satisfy the growing energy demand with more efficient and sustainable energy production processes. SOFCs are electrochemical devices that transform chemical into electrical energy in a direct way, which gives high efficiency (>40%). Besides, they can use a great variety of fuels such as hydrocarbons, alcohols and hydrogen, making them a very versatile device [1].

In a SOFC, oxygen from the gaseous phase is electrochemically reduced to O<sup>2-</sup> ions in the cathode. These ions

diffuse through the electrolyte reaching the anode where they are used to oxidize the fuel to produce H<sub>2</sub>O, CO<sub>2</sub> (if carbon is present in the fuel) and electrons. These electrons go through the external circuit to the cathode. The electrochemical reaction at each electrode takes place in the Three Phase Boundary (TPB) where the gaseous phase, the electrolyte and the electrode converge [2].

Hydrogen has been considered a promising fuel for SOFCs because it is easily electro-oxidized and the resulting product (H<sub>2</sub>O) is environmentally friendly. Nevertheless, it is worth to mention that hydrogen is not a primary source of energy and must be obtained from steam reforming of fossil fuels or biomass, which could be performed directly in the anodic

\* Corresponding author. Departamento de Ingeniería Química, Facultad de Ingeniería, Universidad de Buenos Aires, Pabellón de Industrias, Ciudad Universitaria, 1428 Buenos Aires, Argentina. Tel.: +54 11 47098158.

E-mail addresses: [susana@di.fcen.uba.ar](mailto:susana@di.fcen.uba.ar), [sushilarrondo@yahoo.com.ar](mailto:sushilarrondo@yahoo.com.ar) (S.A. Larrondo).

0360-3199/\$ – see front matter Copyright © 2013, Hydrogen Energy Publications, LLC. Published by Elsevier Ltd. All rights reserved.

<http://dx.doi.org/10.1016/j.ijhydene.2013.12.035>

chamber (internal reforming) due to the high temperature usually used (close to 1000 °C) in the developed prototypes. Despite the possibility to perform internal reforming, such high temperature noticeably reduces the cell lifetime, mainly due to degradation of materials. As a consequence, costly materials are required to avoid these undesirable side-effects. Therefore, decreasing the operating temperature of SOFCs is required for this technology to be economically feasible. The reduction in the operating temperature has a negative effect on electrode kinetics, being important to increase the number of active sites on the electrode surface and to enhance the catalytic activity particularly when hydrocarbons are used as fuel. In this context, nanomaterials exhibiting higher specific surface area, higher porosity and increased grain boundary ionic conductivity have a large potential.

The development of cathodes and electrolytes for SOFCs working at intermediate temperature (550 °C–750 °C) has been reported. Nevertheless, the development of anodes suitable for operating at lower temperatures still remains a challenge [1].

The anode material for Intermediate Temperature SOFCs (IT-SOFCs) has to fulfill some requirements like high porosity to allow gaseous phase to flow to and from TPB, excellent electronic conductivity to collect the electrons released in the reaction and high catalytic activity when hydrocarbons are used as fuel [3]. At intermediate temperature, materials with both electronic and ionic conductivity are highly desirable since they allow the direct feeding of hydrocarbons. These materials will be able to provide oxide ions ( $O^{2-}$ ) to the reaction sites and to transport the electrons ( $e^-$ ) released by the oxidation reaction, allowing the fuel oxidation to take place over the entire surface of the electrode. Besides, anode materials with outstanding catalytic activity to convert the fuel into CO and  $H_2$  mixtures that are easily electro-oxidized to  $CO_2$  and  $H_2O$  are highly convenient [4].

Ceria ( $CeO_2$ )–Zirconia ( $ZrO_2$ ) mixed oxides have been intensely studied due to their redox properties and oxygen storage capacity [5–7]. In fact, these oxides present mixed ion-electronic conductivity in reducing atmospheres and are suitable for anode requirements in cermets with an appropriate amount of metallic phase [4,8]. Particularly,  $Ce_{0.9}Zr_{0.1}O_2$  (ZDC) has shown an excellent performance as a catalyst for Total Oxidation of Methane (TOM) as well as a support for Ni-based catalysts for Catalytic Partial Oxidation of Methane (CPOM) [6,7,9]. NiO(60 wt.%)/ZDC cermets were prepared and tested as anode of IT-SOFCs exhibiting a promising performance [8]. It is worth to mention that increasing Ni loadings significantly contribute to carbon filament formation when hydrocarbons are used as fuel, being the Ni particles the nucleation centers for carbonaceous residues to grow [11].

As a consequence, one of the strategies to reduce carbon deposition is to use bimetallic catalysts, like Ni–Cu/ZDC, due to the fact that Cu has proven to have no tendency towards carbon deposition and presented enhanced reducibility properties, which could be beneficial to the Ni/ZDC system [10].

Song et al. [12] studied the fuel cell electrochemical performance using different bimetallic Cu–Ni anode materials supported over  $Ce_{0.9}Zr_{0.1}O_2$ . The best performance was obtained with  $Ni_{0.5}Cu_{0.5}/Ce_{0.9}Zr_{0.1}O_2$  anode fed with a humidified

flow of 97 mol%  $CH_4$  (3 mol%  $H_2O$ ). Nevertheless, no detailed studies have been performed to assess the effect of adding Cu to the redox and catalytic properties, particularly if high metal loadings are required.

In this work, the catalytic performance of Ni–Cu/ $Ce_{0.9}Zr_{0.1}O_2$  materials in reducing conditions (excess of methane) is presented. The effect of Ni substitution by Cu in the Ni/ $Ce_{0.9}Zr_{0.1}O_2$  solid on the catalytic activity, morphological structure, tendency towards coke deposition and electrochemical performance is also discussed.

## 2. Experimental

### 2.1. Catalyst preparation

The  $Ce_{0.9}Zr_{0.1}O_2$  (ZDC) was synthesized by the glycine/nitrate combustion process, previously reported elsewhere [13,14]. The synthesized solid was calcined at 600 °C for 2 h in order to eliminate carbonaceous residues. Impregnation of Cu and/or Ni was carried out through the incipient wetness method from the corresponding nitrate dissolved in ethanol solutions. Afterwards, the resulting material was calcined for 2 h at 1000 °C. The following samples were prepared: (Cu/ZDC: [CuO(60 wt.%)/ZDC]; Ni/ZDC: [NiO (60 wt.%)/ZDC]; CuNi/ZDC: [CuO(30 wt.%)-NiO(30 wt.%)/ZDC]).

### 2.2. Catalyst characterization

BET surface area was evaluated using  $N_2$  physisorption with a Quantachrome Corporation Autosorb-1 equipment. Samples were previously degassed with He at 50 °C for 24 h. Results were obtained using the five point BET method.

Solid structure was studied with X-Ray Powder Diffraction (XPD) technique, using a Phillips PW3710 diffractometer operated with Cu- $K_{\alpha}$  radiation and a graphite monochromator. Data was collected in the angular region of  $2\theta = 20$ – $80^\circ$  with a step size of  $0.03^\circ$  and a time per step of 4 s.

Temperature Programmed Reduction (TPR) experiments were performed in a Micromeritics Chemisorb 2720 equipment using a heating ramp of  $10^\circ C \text{ min}^{-1}$  in a flow consisting of 5 mol%  $H_2$  in Ar ( $50 \text{ cm}^3(\text{STP}) \text{ min}^{-1}$ ). The experiments started at room temperature and finished at 900 °C. Prior to each measurement, the sample was pre-treated by heating with a rate of  $10^\circ C \text{ min}^{-1}$  in pure He flow to 300 °C, staying at this temperature for 1 h and cooling down to ambient temperature. The pre-treatment was performed in order to eliminate any compound that might have been adsorbed in the solid surface. The equipment determines the  $H_2$  uptake with a Thermal Conductivity Detector (TCD) previously calibrated.

### 2.3. Catalytic activity tests

Catalytic experiments were performed in a conventional quartz fixed-bed reactor operated isothermally, at atmospheric pressure, externally heated by an electric oven provided with a temperature controller. Temperature measurements were registered by means of a thermocouple axially inserted in the center of the catalytic bed.

In all experiments the catalytic mass was of 49.5 mg diluted with inert material in a 1:6 mass ratio to prevent the formation of hot spots. Total feed flow in the reactor was of  $439 \text{ cm}^3(\text{STP}) \text{ min}^{-1}$  with the following composition: 3.1 mol%  $\text{CH}_4$ , 1.2 mol%  $\text{O}_2$  and  $\text{N}_2$  balance (molar feed ratio  $\text{CH}_4:\text{O}_2 = 2.6$ ). Note that excess methane was selected in order to observe the catalyst performance in a reducing atmosphere. Tests were performed in a temperature range of  $300 \text{ }^\circ\text{C}$ – $750 \text{ }^\circ\text{C}$ .

Feed and exit compositions were determined by on-line gas chromatography with an HP 6890+ gas chromatographer equipped with a CTR1 column and a TCD, using He as a carrier.

Thermal stability was assessed in typical 8 h on-stream experiments at  $750 \text{ }^\circ\text{C}$  to evaluate carbon deposition and evolution of catalytic activity.

Results are presented as:

$$\text{CH}_4 \text{ Conversion : } \%X_{\text{CH}_4} = \frac{\text{CH}_4^{\text{in}} - \text{CH}_4^{\text{out}}}{\text{CH}_4^{\text{in}}} \cdot 100$$

$$\text{CO Selectivity : } \%S_{\text{CO}} = \frac{\text{CO}^{\text{out}}}{\text{CH}_4^{\text{in}} - \text{CH}_4^{\text{out}}} \cdot 100$$

$$\text{CO}_2 \text{ Selectivity : } \%S_{\text{CO}_2} = \frac{\text{CO}_2^{\text{out}}}{\text{CH}_4^{\text{in}} - \text{CH}_4^{\text{out}}} \cdot 100$$

$$\text{H}_2 \text{ Selectivity : } \%S_{\text{H}_2} = \frac{\text{H}_2^{\text{out}}}{2(\text{CH}_4^{\text{in}} - \text{CH}_4^{\text{out}})} \cdot 100$$

where  $\text{CH}_4^{\text{in}}$  represents the methane molar flow in the feed,  $\text{CH}_4^{\text{out}}$  the methane molar flow in the exit,  $\text{CO}^{\text{out}}$  the carbon monoxide molar flow in the exit,  $\text{CO}_2^{\text{out}}$  the carbon dioxide molar flow in the exit and  $\text{H}_2^{\text{out}}$  the hydrogen molar flow in the exit. It is important to note that water produced in the reaction is absorbed in a silica-gel fixed bed in the reactor outlet.

#### 2.4. Symmetric cell assembly and electrochemical evaluation

The symmetric cell [anode/electrolyte/anode] was built over electrolyte disks of 10 mol% $\text{Sm}_2\text{O}_3$ – $\text{CeO}_2$  (SDC) provided by Fuel Cells Materials. The disks were prepared by uniaxial pressing of the SDC powder at  $1.5 \text{ ton cm}^{-2}$  in specially designed matrices and afterwards sintered at  $1450 \text{ }^\circ\text{C}$  for 2 h with heating and cooling ramps of  $5 \text{ }^\circ\text{C min}^{-1}$ . The diameter and thickness of the sintered disks were 16 mm and 0.7 mm respectively. The CuNi/ZDC anode powder was mixed with a liquid binder (Decoflux™ WB41, Zschwimmer and Schwartz) obtaining a slurry that was deposited on both sides of the SDC disks by the thick-film technique. The cells were then dried at  $90 \text{ }^\circ\text{C}$  and sintered at high temperature in order to get a good adhesion of the coating to the electrolyte disk. Three different sintering temperatures  $900 \text{ }^\circ\text{C}$ ,  $950 \text{ }^\circ\text{C}$  and  $1000 \text{ }^\circ\text{C}$  were selected in order to analyze the influence of sintering temperature on the anode polarization resistance. Afterwards, a thin layer of Pt conductive ink fired at  $850 \text{ }^\circ\text{C}$  for 30 min was deposited on top of the anode to act as current collector. Symmetric cell experiments were carried out in a lab-designed device suitable for performing experiments in different atmospheres.

The anode polarization resistance was determined by Electrochemical Impedance Spectroscopy (EIS) technique performed with an Autolab PG-GT with frequency analyzer. The experiments were performed with 20 mV of AC perturbation, in the 1 MHz to 0.01 Hz frequency domain. The impedance spectra were collected at isothermal conditions, beginning at  $750 \text{ }^\circ\text{C}$  and cooling down to  $600 \text{ }^\circ\text{C}$  in  $50 \text{ }^\circ\text{C}$  steps. At each temperature the dwell time was large enough to assure thermal stability and good repeatability. Feed gases were supplied at a constant flow of  $80 \text{ cm}^3(\text{STP}) \text{ min}^{-1}$  and relative humidity of 3 mol%. Feed compositions were 7 mol%  $\text{H}_2$  ( $\text{N}_2$  balance) and 5 mol%  $\text{CH}_4$  ( $\text{N}_2$  balance). All gas flows were monitored by mass-flow controllers. The total electrode polarization resistance ( $R_p$ ) was directly measured from the differences between the low and high frequency intercepts with the real axis on the impedance Nyquist plot. The area-specific resistance (ASR) of the electrode was calculated as:  $\text{ASR} = 0.5 R_p A_e$ , where  $A_e$  is the electrode area.

### 3. Results and discussion

#### 3.1. Characterization

BET surface area results are presented in Table 1. ZDC samples after synthesis presented a specific surface area of  $51 \text{ m}^2 \text{ g}^{-1}$ , while after calcination at  $600 \text{ }^\circ\text{C}$  it was reduced to  $40 \text{ m}^2 \text{ g}^{-1}$ , making evident the effect of calcination temperature in the reduction of specific surface area. High metal loading (60 wt%), altogether with elevated calcination temperature resulted in a significant reduction of surface area to values as  $2.7 \text{ m}^2 \text{ g}^{-1}$  for the Cu/ZDC catalyst.

In Fig. 1 the TPR profile of ZDC support is plotted. The presence of the  $\text{Ce}^{4+}/\text{Ce}^{3+}$  redox couple in the ZDC solid is responsible for the redox properties and the intense use of  $\text{CeO}_2$ – $\text{ZrO}_2$  mixed oxides in catalysis. The TPR profile of these mixed oxides depends on four main subjects: the thermodynamic and the kinetics of the reduction process, the textural changes due to sintering (caused by combining effects of atmosphere and temperature) and diffusion phenomena inside the material (oxygen diffusion in the lattice) [15]. In Fig. 1, it is possible to see two peaks at  $530 \text{ }^\circ\text{C}$  and  $725 \text{ }^\circ\text{C}$  respectively. The first peak is usually ascribed to the reduction of cerium surface species while the second one to the reduction of bulk cerium sites [15]. The  $\text{H}_2$  uptake per gram (Table 1) corresponds to a 43.1% reduction of cerium sites.

In Fig. 2 the reduction profiles of Cu/ZDC, Ni/ZDC and CuNi/ZDC samples calcined at  $350 \text{ }^\circ\text{C}$  and  $1000 \text{ }^\circ\text{C}$  were plotted together with those of CuO and NiO. The reduction profile of both Cu/ZDC samples moved to lower temperature respect to that of the corresponding CuO, indicating the beneficial effect

**Table 1 – BET surface area and  $\text{H}_2$  uptake.**

Sample	Calcination temperature ( $^\circ\text{C}$ )	Specific area ( $\text{m}^2 \text{ g}^{-1}$ )	$\text{H}_2$ uptake ( $\text{ml g}^{-1}$ )
ZDC	600	40	28
Cu/ZDC	1000	2.7	193
Ni/ZDC	1000	8.1	200
CuNi/ZDC	1000	3.7	196

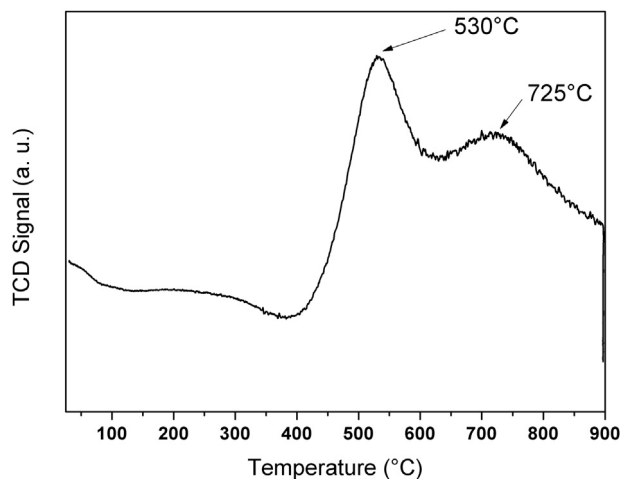


Fig. 1 – TPR profile of ZDC support.

of dispersion on reducibility. The calcination temperature showed the opposite effect due to grain growth. This tendency could also be observed for Ni/ZDC solids, while in CuNi/ZDC sample is less evident.

In Fig. 3, the TPR results for Cu/ZDC, Ni/ZDC and CuNi/ZDC samples calcined at 1000 °C are depicted together. All the solids showed two peaks being confirmed that the more intense one is mainly related with the reduction of metal oxide, due to the high metal loading on the samples (60 wt.%), while the second one to the bulk ceria sites [16]. The second peak is less intense and for that reason it is shown enlarged in the inset. Then, in Cu/ZDC solid the first peak describes the transition  $\text{Cu}^{2+} \rightarrow \text{Cu}^+ \rightarrow \text{Cu}^0$  and the second one the  $\text{Ce}^{4+} \rightarrow \text{Ce}^{3+}$ .

The Ni/ZDC catalyst presented a broad reduction profile at a higher temperature range: 330 °C–760 °C with two unresolved peaks with maxima at 405 °C and 520 °C. It is widely considered that low temperature peaks are related to relatively free NiO species, while high temperature peaks are associated to NiO species that strongly interact with the support. This strong interaction enhances ceria reducibility, most probably due to enhancement of oxygen mobility in the Ce–Zr support [6,17]. On the other hand, CuNi/ZDC catalyst exhibited two main reduction peaks at intermediate temperatures (274 °C and 338 °C) suggesting that the addition of Cu to the solid strongly promotes Ni reduction. These results are in agreement with those reported by Rogatis et al. [10].

TPR peak integration results are informed in Table 1. All samples presented similar reducibility properties with no significant differences in the values of  $\text{H}_2$  uptake. Therefore, the addition of Cu shifts the reduction profile to lower temperatures without modifying significantly the  $\text{H}_2$  consumption.

XRD patterns for fresh (F), used (S) samples after catalytic tests and samples after TPR experiments (TPR) are presented in Fig. 4. The pattern corresponding to the cubic fluorite type structure of Ce–Zr support (ZDC) is present in all the diffractograms. In Ni/ZDC F solids the main peaks of NiO could be observed, while in Ni/ZDC S those corresponding to Ni<sup>0</sup> with small amounts of NiO. This result is indicating that NiO is

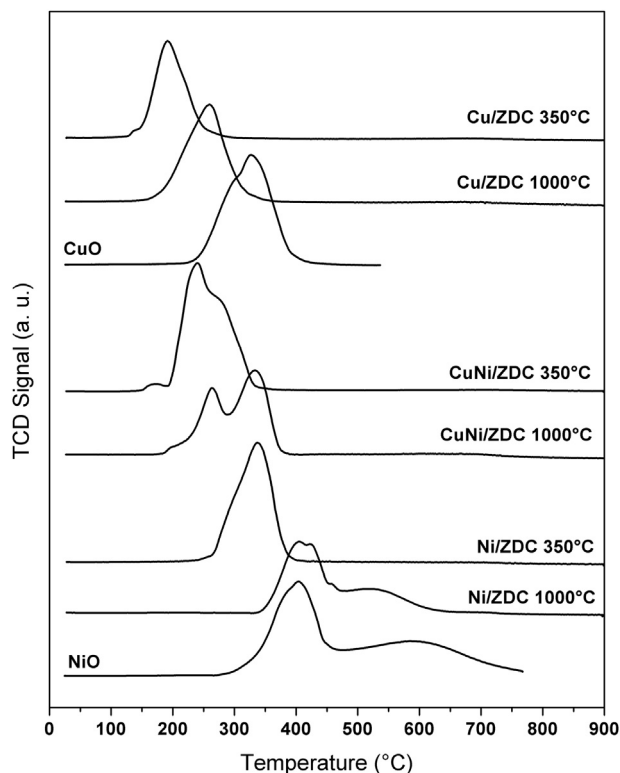


Fig. 2 – TPR profiles of Cu/ZDC, Ni/ZDC and CuNi/ZDC samples calcined at 350 °C and 1000 °C; TPR profiles of pure NiO and CuO.

partially reduced in the reaction atmosphere with excess of methane. At  $2\theta = 26.3^\circ$  an intense peak corresponding to carbon can be observed, indicating that carbon deposition occurred on the catalyst surface during the catalytic tests. Regarding Cu/ZDC catalyst, CuO peaks are visible in the fresh sample whereas for the used one Cu<sup>0</sup>, CuO and Cu<sub>2</sub>O peaks are observed. For CuNi/ZDC solids, the main peaks corresponding to CuO and NiO are present separately in the fresh sample. In

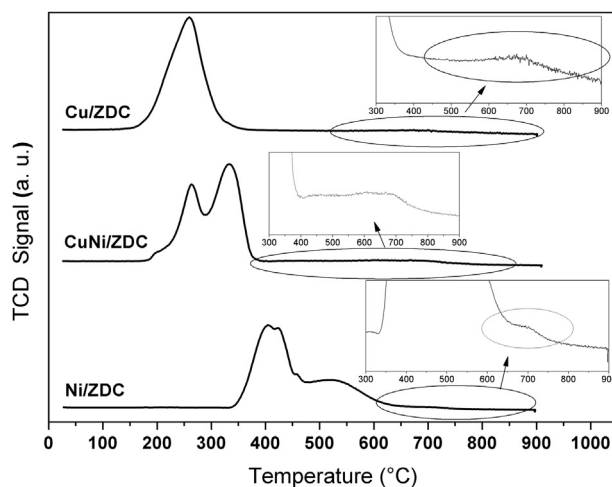


Fig. 3 – TPR profiles of Cu/ZDC, Ni/ZDC and CuNi/ZDC calcined at 1000 °C.

the spent catalysts, the peaks corresponding to  $\text{Cu}^\circ$  and  $\text{Ni}^\circ$  become partially overlapped evidencing the formation of a CuNi alloy. There is only a few evidence of carbon deposition with a carbon peak of very low intensity. XRD profiles for TPR samples exhibit the ZDC phase from the support. Cu and Ni containing catalysts present peaks corresponding to  $\text{Cu}^\circ$  and  $\text{Ni}^\circ$ , respectively. For the bimetallic sample, CuNi alloy peaks can be observed in between the pure  $\text{Ni}^\circ$  and  $\text{Cu}^\circ$  peak positions.

### 3.2. Catalytic activity

Fig. 5 presents  $\text{CH}_4$  conversion for Ni/ZDC and CuNi/ZDC samples evaluated in a wide range of temperatures: 300 °C–750 °C. In all cases, an increase in conversion with temperature was evidenced. Prior to conducting a detailed analysis of the results, it is important to point out that the  $\text{CH}_4/\text{O}_2$  ratio used was 2.6, clearly indicating that  $\text{O}_2$  is the limiting reactant throughout the course of the reaction. Therefore, if we consider that CPOM is the only reaction taking place, the maximal theoretical methane conversion is 76.9% according to the stoichiometry of the reaction.

Cu/ZDC catalyst was only active for Total Oxidation of Methane (TOM) throughout the whole analyzed temperature range, producing only  $\text{H}_2\text{O}$  and  $\text{CO}_2$ , with 100% selectivity to  $\text{CO}_2$ . Conversion reached its maximum of 15.7% at 750 °C and no complete oxygen conversion was detected at any temperature. High CuO loadings are responsible for the formation of bulk CuO, which is responsible for such low catalytic activity. Catalysts containing Cu are not active for CPOM as they do not catalyze the methane decomposition reaction [18]. Park et al.

[19] studied Cu/ $\text{Al}_2\text{O}_3$  catalysts to assess the effect of Cu loading in their structure and catalytic activity. Less than 5% CuO loadings lead to a highly dispersed phase and loadings surpassing 8% CuO led to the formation of big CuO crystallites, responsible for the decrease in catalytic activity.

Nevertheless, it is important to point out that the support (ZDC) is active for TOM. Zimic et al. [13] obtained 85% methane conversion for the support at 750 °C. Therefore, activity for the Cu/ZDC sample may not be only due to the presence of CuO but also due to the presence of the ZDC.

Ni/ZDC sample was highly active and selective for CPOM with a steep jump in conversion from 1.6% at 670 °C to 74% at 720 °C. This abrupt variation is consistent with NiO reduction in the catalyst and it is related to the mechanism by which the methane molecule decomposes over the solid surface. One of the mechanisms proposed [20] for methane decomposition over Ni catalysts is the one that establishes that at low temperatures TOM takes place, followed by steam and  $\text{CO}_2$  methane reforming on reduced Ni sites ( $\text{Ni}^\circ$ ). Methane decomposition takes place over  $\text{Ni}^\circ$  sites and oxygen for the reaction can be supplied either by the gas phase mixture or by oxygen from the ZDC lattice. Coexistence of NiO and  $\text{Ni}^\circ$  can be corroborated in the XRD diffraction pattern where both species can be found after performing catalytic tests. The high calcination temperature selected promotes sintering, turning more difficult the reduction process. Reduction takes place at a critical temperature, where there is a conversion leap that is highly dependent of the calcination temperature and the metal loading. Larrondo et al. [9] studied methane decomposition over Ni/ZDC catalysts and conversion leap was found to take place at higher temperatures for 50%Ni/ZDC catalysts compared to the 9%Ni/ZDC ones. This accounts for the higher activation temperatures observed in this study. CuNi/ZDC sample presented 36% methane conversion at 750 °C. The main difference between this catalyst and the former ones is the coexistence of both TOM and CPOM.

In Fig. 6 selectivity to CO and  $\text{CO}_2$  are presented for Ni/ZDC and CuNi/ZDC samples. Ni/ZDC presented 100% selectivity to

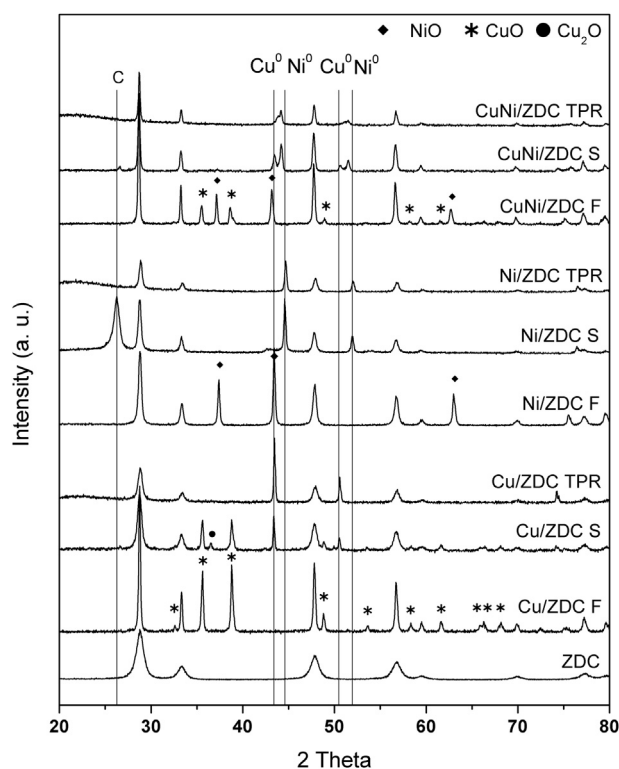


Fig. 4 – XRD diffractograms for samples: fresh (F), after catalytic tests (S) and after TPR experiments (TPR).

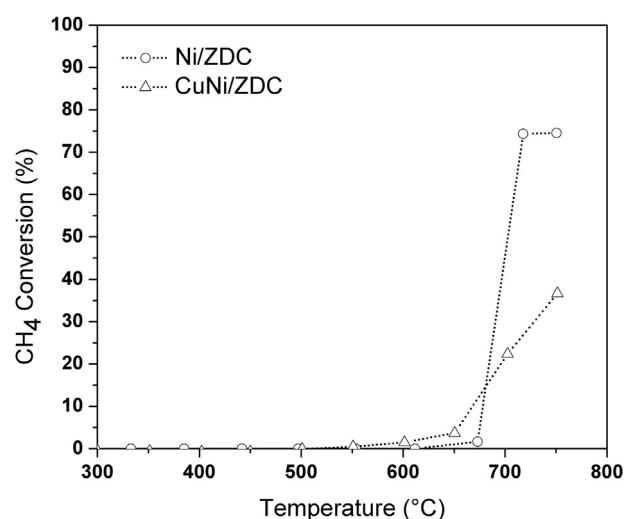


Fig. 5 – Methane conversion vs. temperature for CuNi/ZDC and Ni/ZDC samples calcined at 1000 °C during catalytic tests with  $\text{CH}_4:\text{O}_2$  molar ratio 2.6:1.

CO in the whole range in which the catalyst was active. At temperatures below 700 °C, for the CuNi/ZDC sample, TOM prevailed with a higher selectivity to CO<sub>2</sub> compared to that of CO. However, already at 700 °C and for 750 °C this tendency was reverted and CPOM prevailed with 56% and 77% selectivity to CO for 700 °C and 750 °C respectively.

Fig. 7 presents H<sub>2</sub> selectivity values. Clearly, Ni/ZDC exhibited 100% selectivity to H<sub>2</sub> and CuNi/ZDC presented 55% selectivity at 750 °C.

An important parameter to consider while analyzing product distribution is H<sub>2</sub>:CO molar ratio in the effluent stream. Fig. 8 presents these results. Firstly, for Ni/ZDC catalyst, the relationship remained slightly higher than 2, in the temperature range in which the catalyst was active for CPOM. In contrast, CuNi/ZDC catalyst presented values of 1.2 and 1.5 for 700 °C and 750 °C. Souza et al. [21] suggested that at low temperatures H<sub>2</sub>:CO molar ratio is strongly influenced by the equilibrium of the Reverse Water Gas Shift Reaction (RWGS). A relationship close to 2 is consistent with CPOM stoichiometry. Nevertheless, a considerable amount of reactions take place simultaneously in this system; most of them are reversible reactions, except for oxidations which can generally be considered as irreversible [22]. However, taking into account thermodynamic considerations, only those reactions that present equilibrium constants higher than one will be plausible for a given temperature. One of these reactions is the RWGS that consumes H<sub>2</sub> and CO<sub>2</sub> to produce H<sub>2</sub>O and CO, lowering H<sub>2</sub>:CO ratio. This might explain the low values of H<sub>2</sub>:CO ratio obtained for CuNi/ZDC catalysts. On the other hand, Ni/ZDC catalysts might have exhibited a value higher than 2 as a consequence of methane cracking and Boudouard reactions, both responsible for carbon deposition in the catalyst surface. The first reaction produces H<sub>2</sub> and the second one consumes CO so carbon formation might account for H<sub>2</sub>:CO ratios higher than 2.

Typical 8 h on-stream experiments were carried out on all samples at 750 °C. Methane conversion as a function of time on stream is presented in Fig. 9. CuNi/ZDC proved to be stable with some decrease in activity in the first 50 min of reaction.

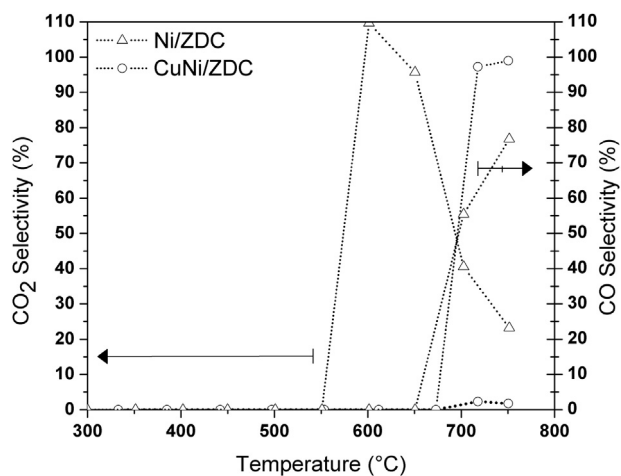


Fig. 6 – CO and CO<sub>2</sub> selectivities vs. temperature for CuNi/ZDC and Ni/ZDC samples calcined at 1000 °C during catalytic tests with CH<sub>4</sub>:O<sub>2</sub> molar ratio 2.6:1.

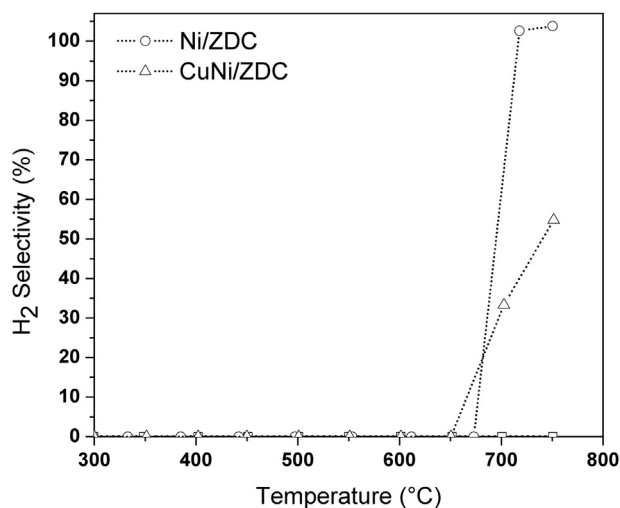


Fig. 7 – H<sub>2</sub> selectivities vs. temperature for CuNi/ZDC and Ni/ZDC samples calcined at 1000 °C during catalytic tests with CH<sub>4</sub>:O<sub>2</sub> molar ratio 2.6:1.

On the contrary, Ni/ZDC presented a considerable decrease in activity in the first 100 min until it reached a value close to 76.9% consistent with maximum theoretical conversion for CPOM with excess methane feed. This means that in the first 100 min excess methane is reacting without any oxygen left, probably following the methane cracking reaction to produce carbon on the catalyst surface.

Carbon balance matched  $100 \pm 3\%$  in all experiments performed for Cu/ZDC and CuNi/ZDC catalysts. Ni/ZDC catalysts exhibited a considerable amount of carbon formation with an overall carbon balance of  $100 \pm 11\%$ .

SEM images of fresh and used samples for Ni/ZDC and CuNi/ZDC are presented in Fig. 10. They reveal the presence of filament-type carbonaceous residues on Ni/ZDC used samples. CuNi/ZDC catalyst exhibited no carbon formation after

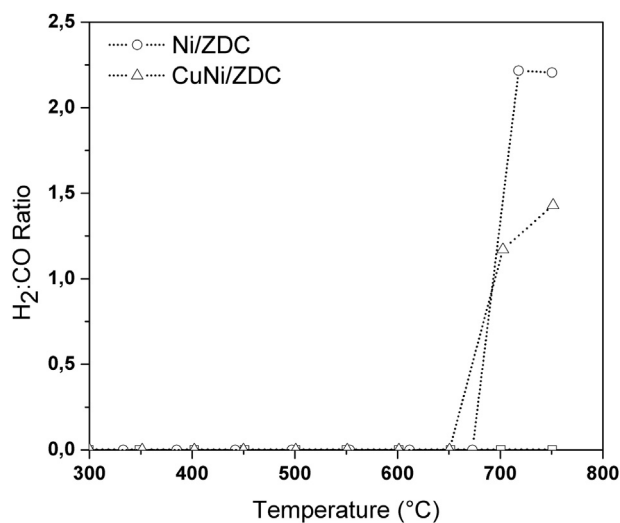


Fig. 8 – H<sub>2</sub> to CO molar ratio in the outlet vs. temperature during catalytic tests with CH<sub>4</sub>:O<sub>2</sub> molar ratio 2.6:1 for CuNi/ZDC and Ni/ZDC samples calcined at 1000 °C.

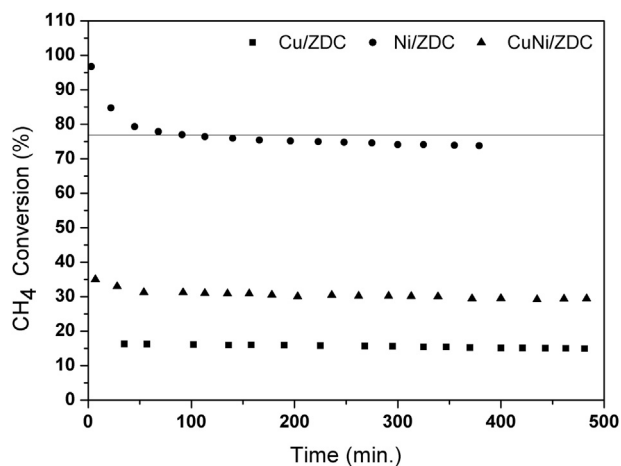


Fig. 9 – Methane conversion vs. time-on stream during stability tests with CH<sub>4</sub>:O<sub>2</sub> molar ratio 2.6:1, at 750 °C, for CuNi/ZDC and Ni/ZDC samples calcined at 1000 °C.

8 h on stream and no carbon formation was observed in Cu/ZDC samples either.

### 3.3. Electrochemical characterization

During the manufacturing process of the symmetric-cell is necessary to select the appropriate temperature to fix the electrode to the electrolyte so as to ensure good adhesion and optimization of the microstructure. Zimicz et al. [8] reported

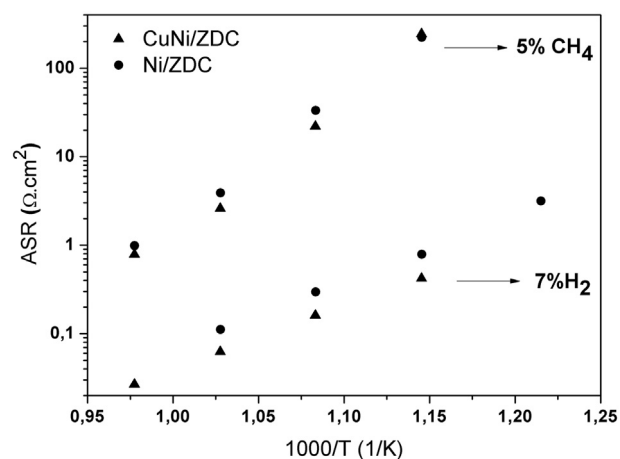


Fig. 11 – Electrocatalytic performance of CuNi/ZDC and Ni/ZDC in symmetrical cell configuration with different atmosphere composition.

an optimum temperature of 1000 °C for Ni/ZDC anodes. In the present work three temperatures were evaluated: 1000 °C, 950 °C and 900 °C. The experiments were performed in a 7 mol % H<sub>2</sub> (N<sub>2</sub> balance) humidified flow (3 mol% H<sub>2</sub>O). The results gave a lower value of ASR for calcination temperature of 950 °C. The results presented hereinafter were obtained with symmetric cells built up with this temperature to fix the anodes.

In Fig. 11 the variation of ASR with temperature for Ni/ZDC anodes (fixed at the optimal temperature determined

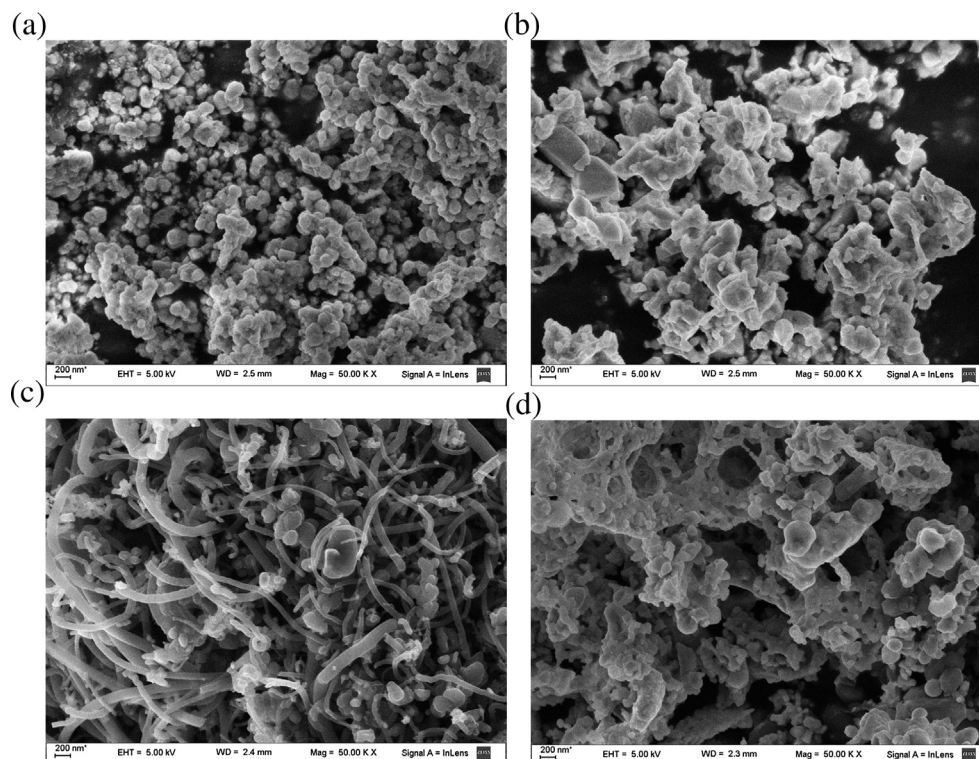


Fig. 10 – SEM images of fresh and used samples (a) fresh Ni/ZDC, (b) fresh CuNi/ZDC, (c) Ni/ZDC after stability test, (d) CuNi/ZDC after stability test.

elsewhere [8]) and CuNi/ZDC anodes (fixed at 950 °C) are plotted. The measurements were performed in two flow compositions consisting of 7 mol% H<sub>2</sub> (He balance) and 5 mol% CH<sub>4</sub> (N<sub>2</sub> balance). It can be seen that bimetallic anode exhibited lower ASR values in all the temperature range (550 °C–750 °C) in both atmospheres.

#### 4. Conclusions

The partial replacement of Ni by Cu to obtain bimetallic cermet with Ce<sub>0.9</sub>Zr<sub>0.1</sub>O<sub>2</sub> mixed oxide was successfully achieved. The CuNi/ZDC samples have shown high reducibility and catalytic performance similar to traditional Ni/ZDC cermet, with stable catalytic activity. Besides, high resistance to carbon deposition after typical 8 h on-stream experiments performed at 750 °C under flows with excess of CH<sub>4</sub> was confirmed by XRD and SEM results. Likewise, an excellent carbon balance matched 100 ± 3% and a H<sub>2</sub>:CO molar ratio lower than 2 are confirmations of that carbon deposition resistance. CuNi/ZDC anode performance observed in the electro-catalytic tests showed a lower polarization resistance than the observed for sample Ni/ZDC evaluated at similar conditions.

These electro-catalytic features combined with good catalytic activity and excellent resistance to the formation of carbonaceous residues make CuNi/ZDC cermets promising anodes for IT-SOFCs.

#### Acknowledgments

The financial support of MINDEF (Miss Lucía Toscani scholarship) and PIDDEF 2011–2013 (N° 011/11), and CONICET (Dr. Zimicz postdoctoral scholarship) is gratefully acknowledged.

#### REFERENCES

- [1] Ruiz Morales JC, Canales Vázquez J, Guerrero López D, Peña Martínez J, Pérez Coll D, Núñez P, et al. *Pilas de Combustible de Óxidos Sólidos (SOFC)*. 1st ed. Tenerife: Centro de la Cultura Popular Canaria; 2008.
- [2] Boudghene Stambouli A, Traversa E. Solid oxide fuel cells (SOFCs); a review of an environmentally clean and efficient source of energy. *Renew Sustain Energy Rev* 2002;6:433–55.
- [3] Chatzichristodoulou C, Blennow PT, Sogaard M, Hendriksen PV, Mogensen MB. Ceria and its use in solid oxide cells and oxygen membranes. In: Trovarelli A, editor. *Catalysis by ceria and related materials*. 2nd ed. London: Imperial College Press; 2013. pp. 623–783.
- [4] Yano M, Tomita A, Sano M, Hibino T. Recent advances in single-chamber solid oxide fuel cells: a review. *Solid State Ionics* 2007;177:3351–9.
- [5] Fornasiero P, Balducci G, Di Monte R, Kaspar J, Sergio V, Graziani M, et al. Modification of the redox behaviour of CeO<sub>2</sub> induced by structural doping with ZrO<sub>2</sub>. *J Catal* 1996;164:173–83.
- [6] Pengpanich S, Meeyoo V, Rirksomboon T. Methane partial oxidation over Ni/CeO<sub>2</sub>–ZrO<sub>2</sub> mixed oxide solid solution catalysts. *Catal Today* 2004;93–95:95–105.
- [7] Larrondo SA, Vidal MA, Irigoyen B, Craievich AF, Lamas DG, Amadeo N, et al. Preparation and characterization of Ce/Zr mixed oxides and their use as catalysts for the direct oxidation of dry CH<sub>4</sub>. *Catal Today* 2005;107:53–9.
- [8] Zimicz MG, Núñez P, Ruiz-Morales JC, Lamas DG, Larrondo SA. Electro-catalytic performance of 60%NiO/Ce<sub>0.9</sub>Zr<sub>0.1</sub>O<sub>2</sub> cermets as anodes of intermediate temperature solid oxide fuel cells. *J Power Sources* 2013;238:87–94.
- [9] Larrondo SA, Kodjaian A, Fábregas I, Zimicz MG, Lamas DG, Amadeo NE, et al. Methane partial oxidation using Ni/Ce<sub>0.9</sub>Zr<sub>0.1</sub>O<sub>2</sub> catalysts. *Int J Hydrogen Energy* 2008;33:3607–13.
- [10] De Rogatis L, Montini T, Cognigni A, Olivi L, Fornasiero P. Methane partial oxidation on NiCu-based catalysts. *Catal Today* 2009;145:176–85.
- [11] Bartholomew CH. Mechanisms of catalyst deactivation. *Appl Catal A* 2001;212:17–60.
- [12] Song S, Han M, Zhang J, Fan H. NiCu–Zr<sub>0.1</sub>Ce<sub>0.9</sub>O<sub>2-d</sub> anode materials for intermediate temperature solid oxide fuel cells using hydrocarbon fuels. *J Power Sources* 2013;233:62–8.
- [13] Zimicz MG, Lamas DG, Larrondo SA. Effect of synthesis conditions on the nanopowder properties of Ce<sub>0.9</sub>Zr<sub>0.1</sub>O<sub>2</sub>. *Mater Res Bull* 2011;46:850–7.
- [14] Zimicz MG, Lamas DG, Larrondo SA. Ce<sub>0.9</sub>Zr<sub>0.1</sub>O<sub>2</sub> nanocatalyst: influence of synthesis conditions in the reducibility and catalytic activity. *Catal Commun* 2011;15:68–73.
- [15] Giordano F, Trovarelli A, De Leitenburg C, Giona M. A model for the temperature-programmed reduction of low and high surface area ceria. *J Catal* 2000;193:273–82.
- [16] Zimicz MG, Larrondo SA, Prado RJ, Lamas DG. Time-resolved in situ XANES study of the redox properties of Ce<sub>0.9</sub>Zr<sub>0.1</sub>O<sub>2</sub> mixed oxides. *Int J Hydrogen Energy* 2012;37:14881–6.
- [17] Roh HS, Jun KW, Dong WS, Chang JS, Park SE, Joe YI. Highly active and stable Ni/Ce–ZrO<sub>2</sub> catalyst for H<sub>2</sub> production from methane. *J Mol Catal A* 2012;181:137–42.
- [18] Gorte RJ, Vohs MJ. Novel SOFC anodes for the direct electrochemical oxidation of hydrocarbons. *J Catal* 2003;216:477–86.
- [19] Park PW, Ledford JS. The influence of surface structure on the catalytic activity of alumina supported copper oxide catalysts. Oxidation of carbon monoxide and methane. *Appl Catal B* 1998;15:221–31.
- [20] Shishido T, Sukenobu M, Morioka H, Kondo M, Wang Y, Takehira K, et al. Partial oxidation of methane over Ni/Mg–Al oxide catalysts prepared by solid phase crystallization method from Mg–Al hydrotalcite-like precursors. *Appl Catal A* 2002;223:35–42.
- [21] Souza M, Schmal M. Combination of carbon dioxide reforming and partial oxidation of methane over supported platinum catalysts. *Appl Catal A* 2003;255:83–92.
- [22] Enger BC, Lødeng R, Holmen A. A review of catalytic partial oxidation of methane to synthesis gas with emphasis on reaction mechanisms over transition metal catalysts. *Appl Catal A* 2008;346:1–27.